Gravity-Driven Flow Over a Porous Inclined Surface

by

Jon-Paul Mastrogiacomo

A research report
presented to the University of Waterloo
in fulfillment of the
research requirement for the degree of
Master of Mathematics
in
Computational Mathematics

Waterloo, Ontario, Canada, 2020

Author's Declaration

I hereby declare that I am the sole author of this research report. This is a true copy of the report, including any required final revisions, as accepted by my examiners.

I understand that my report may be made electronically available to the public.

Abstract

The two-dimensional problem of gravity-driven flow of a thin layer of fluid down a porous inclined surface is discussed. A velocity profile based on the steady-state flow is used to derive a first-order Integrated Boundary Layer model. A linear stability analysis is conducted while non-linear numerical simulations are used to validate the stability predictions. The stability predictions of the first-order model are also compared directly to those of a second-order model. The influence of porosity and other flow parameters is investigated both analytically and numerically.

Acknowledgements

Table of Contents

List of Figures

List of Tables

Chapter 1

Introduction

Gravity-driven flow down an incline is a classic problem in theoretical and experimental fluid mechanics, but also has broad applications in engineering and science. We are interested in what the flow looks like, how it evolves, and whether or not it is stable. That is, if we introduce a small perturbation, will it grow in time or will the flow return to steady-state. This problem has been studied for over sixty years using a variety of tools and techniques [1]-[8]. But the problem also has many well-studied variations with rich dynamics. Some examples include the introduction of a heated boundary, bottom topography, and chemical additives [9]-[16]. In this work we are mainly interested in the case with a porous boundary [15]-[17]. We will investigate how porosity affects the flow and whether it has a stabilizing or destabilizing effect.

The full Navier-Stokes equations and boundary conditions are far too difficult to work with analytically or numerically. Instead, we will develop the Integrated Boundary Layer (IBL) model by integrating across the fluid layer. This reduces the number of flow variables and incorporates the boundary conditions into the governing equations. It results in a system that we can linearize and predict the point of destabilization. The parameter that will control stability will be the Reynolds number, which is usually associated with turbulence. Although our model will not capture the turbulence one would observe in an actual experiment, the Reynolds number will still have an effect that we are familiar with. A large Reynolds number will result in more disturbances with less resemblance to laminar flow. We will simulate our model numerically in Python and compare it to our theoretical predictions.

Chapter 2

Model Development

2.1 Governing Equations and Velocity Profile

Consider the two-dimensional (2D) isothermal flow of a viscous incompressible Newtonian fluid down a porous incline as shown in Figure 2.1.
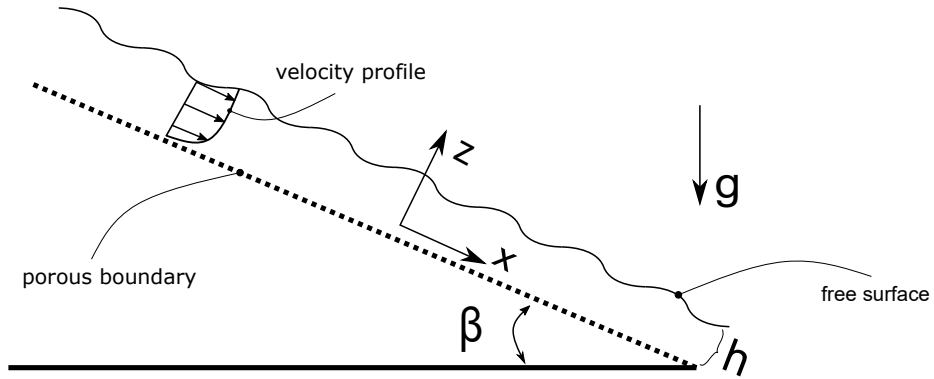

Figure 2.1: 2-D flow down porous incline

We define our coordinate system with x along the incline and z pointing into the fluid layer. Let h denote the fluid thickness, β the angle of inclination, and g the acceleration

due to gravity. The governing Navier-Stokes equations [18] are

$$\frac{\partial u}{\partial t} + u\frac{\partial u}{\partial x} + w\frac{\partial u}{\partial z} = -\frac{1}{\rho}\frac{\partial P}{\partial x} + g\sin\beta + \nu\left(\frac{\partial^2 u}{\partial x^2} + \frac{\partial^2 u}{\partial z^2}\right), \qquad (2.1.1)$$

$$\frac{\partial w}{\partial t} + u\frac{\partial w}{\partial x} + w\frac{\partial w}{\partial z} = -\frac{1}{\rho}\frac{\partial P}{\partial z} - g\cos\beta + \nu\left(\frac{\partial^2 w}{\partial x^2} + \frac{\partial^2 w}{\partial z^2}\right), \qquad (2.1.2)$$

$$\frac{\partial u}{\partial x} + \frac{\partial w}{\partial z} = 0. \qquad (2.1.3)$$

Here u and w are the velocities in the x and z direction respectively, P is the pressure, ρ is the density, and ν is the kinematic viscosity.

2.1.1 Velocity Profile

The first step to understanding this system is to derive a velocity profile of the fluid. We simplify this system by assuming steady, laminar unidirectional flow in the x direction, then

$$\frac{\partial}{\partial t} = 0 \quad \text{and} \quad \frac{\partial}{\partial x} = 0.$$

From equation 2.1.3 we have

$$\frac{\partial w}{\partial z} = 0 \implies w = \text{constant}.$$

But if the surface is sufficiently saturated then a valid approximation is to take $w = 0$. From equation 2.1.2 we get

$$0 = -\frac{1}{\rho}\frac{\partial P}{\partial z} - g\cos\beta,$$

$$\implies \frac{\partial P}{\partial z} = -\rho g\cos\beta,$$

$$\implies P(z) = -\rho g\cos\beta z + \text{constant}.$$

On the free surface we have $P = P_{\text{atm}}$, which gives us the equation for hydrostatic pressure

$$P(z) = P_{\text{atm}} + \rho g\cos\beta(h - z).$$

From equation 2.1.1 we have

$$0 = g \sin \beta + \nu \frac{\partial^2 u}{\partial z^2} \implies \frac{\partial^2 u}{\partial z^2} = -\frac{g \sin \beta}{\nu},$$

which we integrate once to get

$$\frac{\partial u}{\partial z} = -\frac{g \sin \beta}{\nu} z + c_1.$$

Now we apply the zero-stress boundary condition $\frac{\partial u}{\partial z} = 0$ at $z = h$ so that

$$0 = -\frac{g \sin \beta}{\nu} h + c_1,$$

$$\implies c_1 = \frac{g \sin \beta}{\nu} h,$$

and

$$\frac{\partial u}{\partial z} = \frac{g \sin \beta}{\nu} (h - z).$$

We integrate again and get

$$u(z) = \frac{g \sin \beta}{2\nu} z(2h - z) + c_2.$$

We need this to obey the porous bottom boundary condition $u = \delta_1 \frac{\partial u}{\partial z}$ at $z = 0$ from [7] & [19]. This will be further explained in section 2.2. Note that

$$u(0) = c_2,$$

so

$$c_2 = \delta_1 \left. \frac{\partial u}{\partial z} \right|_{z=0},$$

$$= \delta_1 \frac{g \sin \beta}{2\nu} \left. (2h - z - z) \right|_{z=0},$$

$$= \frac{g \sin \beta}{2\nu} 2\delta_1 h.$$

Our velocity profile is therefore

$$u(z) = \frac{g \sin \beta}{2\nu} \left[z(2h - z) + 2\delta_1 h \right]. \tag{2.1.4}$$

4

2.1.2 Nondimensionalization

It is extremely useful in the study of fluids to non-dimensionalize the equations that we work with. That way we do not have to be concerned by the units of the flow variables or parameters such as ν. Instead the flow is controlled entirely by unit-less parameters like the Reynolds number or the Weber number. Before we non-dimensionalize, we need one crucial expression that quantifies the amount of fluid flowing down the incline at any point. This is known as the flow rate and we can calculate it from our our velocity profile, so

$$
\begin{aligned}
q &= \int_0^h u \, dz, \\
&= \frac{g \sin \beta}{2\nu} \left[h^3 - \frac{h^3}{3} + 2\delta_1 h^2 \right], \\
&= \frac{g \sin \beta}{3\nu} h^3 \left[1 + \frac{3\delta_1}{h} \right].
\end{aligned}
\tag{2.1.5}
$$

This quantity is typically prescribed in experiments. Now we are ready to decide how to non-dimensionalize the governing Navier-Stokes equations 2.1.1-2.1.3. Instead of using the flow rate based on slip-length, we will use a no-slip flow rate. This is equivalent to setting $\delta_1 = 0$ in 2.1.5. We will denote this no-slip flow rate by Q. Now we rearrange to obtain the expression

$$
H = \left(\frac{3\nu Q}{g \sin \beta} \right)^{\frac{1}{3}}.
\tag{2.1.6}
$$

This is known as the Nusselt thickness and we will use it as our length scale in the z direction. Similarly we choose a length scale L in the x direction and typically we have $L \gg H$. So we define $\delta = \frac{H}{L} \ll 1$ to be the shallowness parameter. Similarly we will choose a velocity scale U and a pressure scale ρU^2. We also have the fact that $Q = HU$. We denote a dimensionless parameter with an asterisk and introduce the following quantities:

$$
x = Lx^*, \quad z = Hz^*, \quad u = Uu^*,
$$
$$
w = W\frac{U}{L}w^*, \quad t = \frac{L}{U}t^*, \quad P = \rho U^2 P^*.
$$

We make the suitable substitutions to equations 2.1.1-2.1.3 so that

$$\frac{U^2}{L}\left(\frac{\partial u^*}{\partial t^*} + u^*\frac{\partial u^*}{\partial x^*} + w^*\frac{\partial u^*}{\partial z^*}\right) = -\frac{U^2}{L}\frac{\partial P^*}{\partial x^*} + g\sin\beta + \nu\left(\frac{U}{L^2}\frac{\partial^2 u^*}{\partial x^{*2}} + \frac{U}{H^2}\frac{\partial^2 u^*}{\partial z^{*2}}\right),$$

$$\frac{U^2 H}{L^2}\left(\frac{\partial w^*}{\partial t^*} + u^*\frac{\partial w^*}{\partial x^*} + w^*\frac{\partial w^*}{\partial z^*}\right) = -\frac{U^2}{H}\frac{\partial P^*}{\partial z^*} - g\cos\beta + \nu\left(\frac{UH}{L^3}\frac{\partial^2 w^*}{\partial x^{*2}} + \frac{U}{LH}\frac{\partial^2 w^*}{\partial z^{*2}}\right),$$

$$\frac{U}{L}\frac{\partial u^*}{\partial x^*} + \frac{U}{L}\frac{\partial w^*}{\partial z^*} = 0.$$

Now we drop the asterisks and use the relations $Q = HU$, $\delta = \frac{H}{L}$, and $Re = \frac{Q}{\nu}$ to get

$$\delta Re\left(\frac{\partial u}{\partial t} + u\frac{\partial u}{\partial x} + w\frac{\partial u}{\partial z}\right) = -\delta Re\frac{\partial P}{\partial x} + H^3\frac{g\sin\beta}{Q\nu} + \delta^2\frac{\partial^2 u}{\partial x^2} + \frac{\partial^2 u}{\partial z^2},$$

$$\delta^2 Re\left(\frac{\partial w}{\partial t} + u\frac{\partial w}{\partial x} + w\frac{\partial w}{\partial z}\right) = -Re\frac{\partial P}{\partial z} - H^3\frac{g\cos\beta}{Q\nu} + \delta^3\frac{\partial^2 w}{\partial x^2} + \delta\frac{\partial^2 w}{\partial z^2},$$

$$\frac{\partial u}{\partial x} + \frac{\partial w}{\partial z} = 0.$$

We use the Nusselt thickness 2.1.6 to arrive at our non-dimensional Navier-Stokes equations

$$\delta Re\left(\frac{\partial u}{\partial t} + u\frac{\partial u}{\partial x} + w\frac{\partial u}{\partial z}\right) = -\delta Re\frac{\partial P}{\partial x} + 3 + \delta^2\frac{\partial^2 u}{\partial x^2} + \frac{\partial^2 u}{\partial z^2}, \qquad (2.1.7)$$

$$\delta^2 Re\left(\frac{\partial w}{\partial t} + u\frac{\partial w}{\partial x} + w\frac{\partial w}{\partial z}\right) = -Re\frac{\partial P}{\partial z} - 3\cot\beta + \delta^3\frac{\partial^2 w}{\partial x^2} + \delta\frac{\partial^2 w}{\partial z^2}, \qquad (2.1.8)$$

$$\frac{\partial u}{\partial x} + \frac{\partial w}{\partial z} = 0. \qquad (2.1.9)$$

The parameter Re is known as the Reynolds number and it will be pivotal to our study of stability in this system. At lower Reynolds numbers the flow tends to be laminar, but a higher value will lead to irregular flow.

Finally we want to non-dimensionalize our flow rate 2.1.5 and our velocity profile 2.1.4 which we will use to develop our model. We choose $q = Qq^*$ and $\delta_1^* = \frac{\delta_1}{H}$ to show that

$$q^* = \frac{g\sin\beta}{3\nu}\frac{H^3}{Q}h^{*3}\left[1 + 3\frac{\delta_1}{Hh^*}\right],$$

$$= \frac{g\sin\beta}{3\nu}\frac{H^3}{Q}h^{*3}\left[1 + 3\frac{\delta_1^*}{h^*}\right].$$

6

Our velocity profile becomes

$$Uu^* = \frac{g\sin\beta}{2\nu}\left[Hz^*(2Hh^* - Hz^*) + 2\delta_1 Hh^*\right],$$

$$\implies \frac{Q}{H}u^* = \frac{g\sin\beta}{2\nu}H^2\left[z^*(2h^* - z^*) + \frac{2\delta_1}{H}h^*\right],$$

$$\implies u^* = \frac{g\sin\beta}{2\nu}\frac{H^3}{Q}\left[z^*(2h^* - z^*) + 2\delta_1^* h^*\right],$$

$$\implies u^* = \frac{3}{2}\frac{q^*}{h^{*3}}\left[\frac{z^*(2h^* - z^*) + 2\delta_1^* h^*}{1 + 3\frac{\delta_1^*}{h^*}}\right].$$

Dropping the asterisks for notational convenience gives us

$$u = \frac{3}{2}\frac{q}{h^3}\left[\frac{z(2h - z) + 2\delta_1 h}{1 + 3\frac{\delta_1}{h}}\right]. \tag{2.1.10}$$

2.2 Boundary Conditions

Before we develop the Integrated Boundary Layer Model we need to prescribe and non-dimensionalize several boundary conditions that define our system.

2.2.1 Porous Bottom

We model a porous boundary with the notion of a slip condition, originally introduced in [7]. To quantify the flow along the boundary, we use the slip length denoted δ_1. This is the distance along the interface where the tangential velocity vanishes, thus becoming no-slip [19]. So at $z = 0$ we have

$$u = \delta_1\frac{\partial u}{\partial z},$$

and we non-dimensionalize so that

$$Uu^* = \delta_1\frac{U}{H}\frac{\partial u^*}{\partial z^*},$$

$$\implies u^* = \delta_1^*\frac{\partial u^*}{\partial z^*}.$$

We drop the asterisk for convenience and get back

$$u = \delta_1 \frac{\partial u}{\partial z}.$$ (2.2.1)

2.2.2 No Normal Flow

Although the boundary is porous, setting $w = 0$ at $z = 0$ is still a valid assumption [15]. After some time the medium past the boundary will become sufficiently saturated to reduce the normal flow to a very small value.

2.2.3 Kinematic Condition

This condition describes the fact that the fluid cannot cross the interface along the free surface. The interface is defined at $z = h(x,t)$. So at $z = h$ we need

$$\frac{D}{Dt}(z - \eta) = 0,$$

$$\implies \frac{Dz}{Dt} - \frac{Dh}{Dt} = 0,$$

$$\implies w = \frac{\partial h}{\partial t} + u\frac{\partial h}{\partial x}.$$

We non-dimensionalize so that

$$U\frac{H}{L}w^* = \frac{H}{L/U}\frac{\partial h^*}{\partial t^*} + Uu^*\frac{H}{L}\frac{\partial h^*}{\partial x^*},$$

$$\implies w^* = \frac{\partial h^*}{\partial t} + u\frac{\partial h^*}{\partial x}.$$

We drop the asterisk and get back

$$w = \frac{\partial h}{\partial t} + u\frac{\partial h}{\partial x}.$$ (2.2.2)

2.2.4 Continuity of Normal and Tangential Stress

We can describe these conditions at the interface $z = h$, as in [12], with the following tensor equations

$$P_{atm} + \hat{\vec{N}} \cdot \tau \cdot \hat{\vec{N}} = -\sigma \vec{\nabla} \cdot \hat{\vec{N}}, \tag{2.2.3}$$

$$\hat{\vec{N}} \cdot \tau \cdot \hat{\vec{T}} = 0. \tag{2.2.4}$$

Here, σ is surface tension, $\hat{\vec{N}}$ is the outward pointing unit normal vector, $\hat{\vec{T}}$ is the unit tangent vector, and τ is the symmetric stress tensor. They are defined as

$$\hat{\vec{N}} = \frac{1}{\sqrt{1 + \left(\frac{\partial h}{\partial x}\right)^2}} \begin{pmatrix} -\frac{\partial h}{\partial x} \\ 1 \end{pmatrix}, \qquad \hat{\vec{T}} = \frac{1}{\sqrt{1 + \left(\frac{\partial h}{\partial x}\right)^2}} \begin{pmatrix} 1 \\ \frac{\partial h}{\partial x} \end{pmatrix},$$

and

$$\tau = \begin{pmatrix} -P + 2\mu\frac{\partial u}{\partial x} & \mu\left(\frac{\partial u}{\partial z} + \frac{\partial w}{\partial x}\right) \\ \mu\left(\frac{\partial u}{\partial z} + \frac{\partial w}{\partial x}\right) & -P + 2\mu\frac{\partial w}{\partial z} \end{pmatrix}.$$

In the stress tensor, μ is called the dynamic viscosity and can be related to the kinematic viscosity through the density: $\nu = \frac{\mu}{\rho}$.

From equation [2.2.4](#), we have

$$0 = \vec{\hat{N}} \cdot \tau \cdot \vec{\hat{T}},$$

$$= \begin{pmatrix} -\frac{\partial h}{\partial x} & 1 \end{pmatrix} \begin{pmatrix} -P + 2\mu\frac{\partial u}{\partial x} & \mu\left(\frac{\partial u}{\partial z} + \frac{\partial w}{\partial x}\right) \\ \mu\left(\frac{\partial u}{\partial z} + \frac{\partial w}{\partial x}\right) & -P + 2\mu\frac{\partial w}{\partial z} \end{pmatrix} \begin{pmatrix} 1 \\ \frac{\partial h}{\partial x} \end{pmatrix},$$

$$= \begin{pmatrix} -\frac{\partial h}{\partial x} & 1 \end{pmatrix} \begin{pmatrix} -P + 2\mu\frac{\partial u}{\partial x} + \mu\frac{\partial h}{\partial x}\left(\frac{\partial u}{\partial z} + \frac{\partial w}{\partial x}\right) \\ \mu\left(\frac{\partial u}{\partial z} + \frac{\partial w}{\partial x}\right) + \frac{\partial h}{\partial x}\left(-P + 2\mu\frac{\partial w}{\partial z}\right) \end{pmatrix},$$

$$= \frac{\partial h}{\partial x}P - 2\mu\frac{\partial u}{\partial x}\frac{\partial h}{\partial x} - \mu\left(\frac{\partial h}{\partial x}\right)^2\left(\frac{\partial u}{\partial z} + \frac{\partial w}{\partial x}\right)$$
$$+ \mu\left(\frac{\partial u}{\partial z} + \frac{\partial w}{\partial x}\right) - \frac{\partial h}{\partial x}P + 2\mu\frac{\partial w}{\partial z}\frac{\partial h}{\partial x},$$

$$= 2\mu\frac{\partial h}{\partial x}\left(\frac{\partial w}{\partial z} - \frac{\partial u}{\partial x}\right) + \mu\left[1 - \left(\frac{\partial h}{\partial x}\right)^2\right]\left(\frac{\partial u}{\partial z} + \frac{\partial w}{\partial x}\right).$$

But we know from the continuity equation [2.1.3](#) that $\frac{\partial w}{\partial z} = -\frac{\partial u}{\partial x}$, so the calculation above reduces to

$$\left[1 - \left(\frac{\partial h}{\partial x}\right)^2\right]\left(\frac{\partial u}{\partial z} + \frac{\partial w}{\partial x}\right) = 4\frac{\partial h}{\partial x}\frac{\partial u}{\partial x}.$$

We non-dimensionalize and get

$$\left[1 - \frac{H^2}{L^2}\left(\frac{\partial h^*}{\partial x^*}\right)^2\right]\left(\frac{U}{H}\frac{\partial u^*}{\partial z^*} + \frac{UH/L}{L}\frac{\partial w^*}{\partial x^*}\right) = 4\frac{H}{L}\frac{\partial h^*}{\partial x^*}\frac{U}{L}\frac{\partial u^*}{\partial x^*}$$

$$\implies \left[1 - \frac{H^2}{L^2}\left(\frac{\partial h^*}{\partial x^*}\right)^2\right]\left(\frac{\partial u^*}{\partial z^*} + \frac{H^2}{L^2}\frac{\partial w^*}{\partial x^*}\right) = 4\frac{H^2}{L^2}\frac{\partial h^*}{\partial x^*}\frac{\partial u^*}{\partial x^*}.$$

Finally dropping the asterisks and using $\delta = \frac{H}{L}$ we have

$$\left[1 - \delta^2\left(\frac{\partial h}{\partial x}\right)^2\right]\left(\frac{\partial u}{\partial z} + \delta^2\frac{\partial w}{\partial x}\right) = 4\delta^2\frac{\partial h}{\partial x}\frac{\partial u}{\partial x}. \qquad (2.2.5)$$

Now we look at equation 2.2.3. Carrying out the matrix multiplication as done above and taking the divergence of the normal vector results in the following

$$0 = P_{atm} + \hat{\vec{N}} \cdot \tau \cdot \hat{\vec{N}} + \sigma \vec{\nabla} \cdot \hat{\vec{N}},$$

$$= P_{atm} + \frac{1}{1 + \left(\frac{\partial h}{\partial x}\right)^2} \left[\left(\frac{\partial h}{\partial x}\right)^2 \left(-P + 2\mu \frac{\partial u}{\partial x}\right) - 2\mu \frac{\partial h}{\partial x}\left(\frac{\partial u}{\partial z} + \frac{\partial w}{\partial x}\right) + \left(-P + 2\mu \frac{\partial w}{\partial z}\right)\right]$$

$$+ \sigma \frac{-\frac{\partial^2 h}{\partial x^2}}{\left[1 + \left(\frac{\partial h}{\partial x}\right)^2\right]^{\frac{3}{2}}},$$

$$= P_{atm} - P + \frac{2\mu}{1 + \left(\frac{\partial h}{\partial x}\right)^2} \left[\frac{\partial u}{\partial x}\left(\frac{\partial h}{\partial x}\right)^2 + \frac{\partial w}{\partial z} - \frac{\partial h}{\partial x}\left(\frac{\partial u}{\partial z} + \frac{\partial w}{\partial x}\right)\right]$$

$$+ \sigma \frac{-\frac{\partial^2 h}{\partial x^2}}{\left[1 + \left(\frac{\partial h}{\partial x}\right)^2\right]^{\frac{3}{2}}}.$$

Again using the fact that $\frac{\partial w}{\partial z} = -\frac{\partial u}{\partial x}$ and rearranging we get

$$P = P_{atm} + \frac{2\mu}{1 + \left(\frac{\partial h}{\partial x}\right)^2} \left[\frac{\partial u}{\partial x}\left(\left(\frac{\partial h}{\partial x}\right)^2 - 1\right) - \frac{\partial h}{\partial x}\left(\frac{\partial u}{\partial z} + \frac{\partial w}{\partial x}\right)\right] - \sigma \frac{\frac{\partial^2 h}{\partial x^2}}{\left[1 + \left(\frac{\partial h}{\partial x}\right)^2\right]^{\frac{3}{2}}}.$$

We always non-dimensionalize to arrive at

$$\rho U^2 P^* = \rho U^2 P_{atm}^*$$

$$+ \frac{2\mu}{1 + \frac{H^2}{L^2}\left(\frac{\partial h^*}{\partial x^*}\right)^2} \left[\frac{U}{L}\frac{\partial u^*}{\partial x^*}\left(\frac{H^2}{L^2}\left(\frac{\partial h^*}{\partial x^*}\right)^2 - 1\right) - \frac{H}{L}\frac{\partial h^*}{\partial x^*}\left(\frac{U}{H}\frac{\partial u^*}{\partial z^*} + \frac{UH}{L^2}\frac{\partial w*}{\partial x^*}\right)\right]$$

$$- \frac{\sigma H}{L^2}\frac{\frac{\partial^2 h^*}{\partial x^{*2}}}{\left[1 + \frac{H^2}{L^2}\left(\frac{\partial h^*}{\partial x^*}\right)^2\right]^{\frac{3}{2}}}.$$

Making some substitutions and dropping the asterisks gives us

$$P = P_{atm} + \left(\frac{\mu}{L\rho U}\right)\frac{2}{1 + \delta^2\left(\frac{\partial h}{\partial x}\right)^2}\left[\frac{\partial u}{\partial x}\left(\delta^2\left(\frac{\partial h}{\partial x}\right)^2 - 1\right) - \frac{\partial h}{\partial x}\left(\frac{\partial u}{\partial z} + \delta^2\frac{\partial w}{\partial x}\right)\right]$$

$$- \left(\frac{\sigma}{\rho H U^2}\right)\frac{\delta^2 \frac{\partial^2 h}{\partial x^2}}{\left[1 + \delta^2\left(\frac{\partial h}{\partial x}\right)^2\right]^{\frac{3}{2}}}.$$

Now we will use the following relationships defined at various points above

$$Q = HU, \qquad \delta = \frac{H}{L}, \qquad \nu = \frac{\mu}{\rho}, \quad \text{and} \quad Re = \frac{Q}{\nu}.$$

We use these to see that

$$\frac{\mu}{L\rho U} = \frac{\mu\delta}{\rho HU} = \frac{\nu\delta}{Q} = \frac{\delta}{Re} \qquad \text{and} \qquad \frac{\sigma}{\rho HU^2} = \frac{\sigma H}{\rho Q^2} = We.$$

Here We is the Weber number and is a measure of surface tension. Finally, we substitute these relationships in to arrive at the final form of the boundary condition

$$P = P_{atm} + \frac{2\delta}{Re\left[1 + \delta^2\left(\frac{\partial h}{\partial x}\right)^2\right]}\left[\frac{\partial u}{\partial x}\left(\delta^2\left(\frac{\partial h}{\partial x}\right)^2 - 1\right) - \frac{\partial h}{\partial x}\left(\frac{\partial u}{\partial z} + \delta^2\frac{\partial w}{\partial x}\right)\right]$$
$$- \frac{We\delta^2\frac{\partial^2 h}{\partial x^2}}{\left[1 + \delta^2\left(\frac{\partial h}{\partial x}\right)^2\right]^{\frac{3}{2}}}. \tag{2.2.6}$$

2.3   Integral Boundary Layer Model

We are now ready to develop the IBL model which is the central idea in this work. Consider the non-dimensional Navier-Stokes equations 2.1.7-2.1.9. In this model we do not work with the full complexity of this system. Instead we will only keep linear terms in δ, dropping all higher order terms. This will result in a simpler model which will be much easier to simulate and study analytically. To first order in δ the equations are

$$\frac{\partial u}{\partial x} + \frac{\partial w}{\partial z} = 0, \tag{2.3.1}$$

$$\delta Re\left(\frac{\partial u}{\partial t} + u\frac{\partial u}{\partial x} + w\frac{\partial u}{\partial z}\right) = -\delta Re\frac{\partial p}{\partial x} + 3 + \frac{\partial^2 u}{\partial z^2}, \tag{2.3.2}$$

$$0 = -Re\frac{\partial p}{\partial z} - 3\cot\beta + \delta\frac{\partial^2 w}{\partial z^2}, \tag{2.3.3}$$

12

with boundary conditions to first order at $z = h$,

$$w = \frac{\partial h}{\partial t} + u\frac{\partial h}{\partial x}, \tag{2.3.4}$$

$$p = p_{atm} - \frac{2\delta}{Re}\left(\frac{\partial u}{\partial x} + \frac{\partial h}{\partial x}\frac{\partial u}{\partial z}\right), \tag{2.3.5}$$

$$0 = \frac{\partial u}{\partial z}, \tag{2.3.6}$$

and at $z = 0$

$$u = \delta_1\frac{\partial u}{\partial z}, \tag{2.3.7}$$

$$w = 0. \tag{2.3.8}$$

In addition to simplifying the governing equations, we will also change the flow variables from u, w, and P to q and h. Here h is just the height of the free surface and q is flow rate defined as $q = \int_0^h u\, dz$. We begin by integrating 2.3.1 across the fluid layer from $z = 0$ to $z = h$, so

$$\int_0^h \frac{\partial u}{\partial x}\, dz + \int_0^h \frac{\partial w}{\partial z}\, dz = 0,$$

$$\implies w|_0^h + \int_0^h \frac{\partial u}{\partial x}\, dz = 0.$$

But using 2.3.4 and 2.3.8 we get

$$\frac{\partial h}{\partial t} + u\frac{\partial h}{\partial x} + \int_0^h \frac{\partial u}{\partial x}\, dz = 0. \tag{2.3.9}$$

By the Leibniz integral integral rule, we know

$$\frac{\partial q}{\partial x} = \frac{\partial}{\partial x}\int_0^h u\, dz,$$

$$= \int_0^h \frac{\partial u}{\partial x}\, dz + u\frac{\partial h}{\partial x},$$

$$\implies \int_0^h \frac{\partial u}{\partial x}\, dz = \frac{\partial q}{\partial x} - u\frac{\partial h}{\partial x}.$$

13

We substitute this into 2.3.9 to find

$$\frac{\partial h}{\partial t} + \frac{\partial q}{\partial x} = 0. \tag{2.3.10}$$

This is the continuity equation expressed in terms of q and h.

Next we seek to eliminate the pressure variable by using 2.3.3. We denote one term as $O(\delta)$ because it will become quadratic in δ as the equations are combined and will be dropped. We begin with

$$\frac{\partial p}{\partial z} = \frac{-3\cot\beta}{Re} + O(\delta).$$

We integrate

$$\int_z^h \frac{\partial p}{\partial z}\,dz = \int_z^h \frac{-3\cot\beta}{Re}\,dz + O(\delta),$$

$$\implies p|_{z=h} - p = \frac{-3\cot\beta}{Re}(h-z) + O(\delta),$$

$$\implies p = p|_{z=h} + \frac{3\cot\beta}{Re}(h-z) + O(\delta),$$

and apply condition 2.3.5

$$p = p_{atm} + \frac{3\cot\beta}{Re}(h-z) + O(\delta).$$

Note that the terms with δ in 2.3.5 have been absorbed in $O(\delta)$. Now we differentiate with respect to x

$$\frac{\partial p}{\partial x} = \frac{3\cot\beta}{Re}\frac{\partial h}{\partial x} + O(\delta),$$

and plug into 2.3.2

$$\delta Re\left(\frac{\partial u}{\partial t} + u\frac{\partial u}{\partial x} + w\frac{\partial u}{\partial z}\right) = -3\cot\beta\frac{\partial h}{\partial x}\delta + 3 + \frac{\partial^2 u}{\partial z^2} + O(\delta^2). \tag{2.3.11}$$

Now we drop the $O(\delta^2)$ term since this is a linear model in δ.

Next we integrate the right-hand side (RHS) of 2.3.11 from 0 to h and use 2.3.6 so that

$$\int_0^h \text{RHS}\, dz = \int_0^h \left(-3\cot\beta \frac{\partial h}{\partial x}\delta + 3 + \frac{\partial^2 u}{\partial z^2} \right) dz,$$

$$= (-3\cot\beta)(\delta h)\frac{\partial h}{\partial x} + 3h + \left.\frac{\partial u}{\partial z}\right|_0^h,$$

$$= (-3\cot\beta)(\delta h)\frac{\partial h}{\partial x} + 3h + 0 - \left.\frac{\partial u}{\partial z}\right|_{z=0}. \qquad (2.3.12)$$

Note that the last term $\left.\frac{\partial u}{\partial z}\right|_{z=0}$ cannot be evaluated. We do not have a boundary condition that covers this case. We leave it for later.

Now before we integrate the left-hand side (LHS) of 2.3.11 we need two facts. First, by the Leibniz integral rule, we know

$$\frac{\partial q}{\partial t} = \frac{\partial}{\partial t}\int_0^h u\, dz,$$

$$= \int_0^h \frac{\partial u}{\partial t}\, dz + u\frac{\partial h}{\partial t},$$

$$\implies \int_0^h \frac{\partial u}{\partial t}\, dz = \frac{\partial q}{\partial t} - u\frac{\partial h}{\partial t}. \qquad (2.3.13)$$

Second, using the fact $\frac{\partial w}{\partial z} = -\frac{\partial u}{\partial x}$ from 2.3.1 we have

$$\int_0^h \left[u\frac{\partial u}{\partial x} + w\frac{\partial u}{\partial z} \right] dz = \int_0^h \left[\frac{1}{2}\frac{\partial u^2}{\partial x} + \frac{\partial uw}{\partial z} - u\frac{\partial w}{\partial z} \right] dz,$$

$$= \int_0^h \left[\frac{1}{2}\frac{\partial u^2}{\partial x} + \frac{\partial uw}{\partial z} + u\frac{\partial u}{\partial x} \right] dz,$$

$$= \int_0^h \left[\frac{1}{2}\frac{\partial u^2}{\partial x} + \frac{\partial uw}{\partial z} + \frac{1}{2}\frac{\partial u^2}{\partial x} \right] dz,$$

$$= \int_0^h \left[\frac{\partial u^2}{\partial x} + \frac{\partial uw}{\partial z} \right] dz. \qquad (2.3.14)$$

We will evaluate this integral in two parts. By the Leibniz integral rule again, we know

$$\int_0^h \frac{\partial u^2}{\partial x}\, dz = \frac{\partial}{\partial x}\int_0^h u^2\, dz - u^2\frac{\partial h}{\partial x}.$$

15

By parts and using 2.3.4 and 2.3.8 we have

$$\int_0^h \frac{\partial uw}{\partial z}\, dz = uw\big|_0^h\,,$$

$$= u\left(\frac{\partial h}{\partial t} + u\frac{\partial h}{\partial x}\right).$$

Combining these with 2.3.14 we have

$$\int_0^h \left[u\frac{\partial u}{\partial x} + w\frac{\partial u}{\partial z}\right]\, dz = \frac{\partial}{\partial x}\int_0^h u^2\, dz - u^2\frac{\partial h}{\partial x} + u\left(\frac{\partial h}{\partial t} + u\frac{\partial h}{\partial x}\right). \qquad (2.3.15)$$

Now we integrate the LHS of 2.3.11 and use 2.3.13 and 2.3.15 to show

$$\int_0^h \text{LHS}\, dz = \delta Re \int_0^h \left(\frac{\partial u}{\partial t} + u\frac{\partial u}{\partial x} + w\frac{\partial u}{\partial z}\right)\, dz,$$

$$= \delta Re \left[\frac{\partial q}{\partial t} - u\frac{\partial h}{\partial t} + \frac{\partial}{\partial x}\int_0^h u^2\, dz - u^2\frac{\partial h}{\partial x} + u\frac{\partial h}{\partial t} + u^2\frac{\partial h}{\partial x}\right],$$

$$= \delta Re \left[\frac{\partial q}{\partial t} + \frac{\partial}{\partial x}\int_0^h u^2\, dz\right].$$

Now that we have the integrals of the LHS and RHS, 2.3.2 becomes

$$\delta Re \left[\frac{\partial q}{\partial t} + \frac{\partial}{\partial x}\int_0^h u^2\, dz\right] = -3\delta h \cot\beta \frac{\partial h}{\partial x} + 3h - \frac{\partial u}{\partial z}\bigg|_{z=0}. \qquad (2.3.16)$$

But now we need to find some way to evaluate $\int_0^h u^2\, dz$ and $\frac{\partial u}{\partial z}\big|_{z=0}$. In order to solve this exactly, we would need the full velocity profile which cannot be solved analytically. Instead we use the velocity profile from section 2.1. Although this was derived using steady unidirectional flow, it is still a valid approximation. Recall the non-dimensional velocity profile 2.1.10

$$u(x, z, t) = \frac{3}{2}\frac{q}{h^3}\left[\frac{z(2h - z) + 2\delta_1 h}{1 + 3\frac{\delta_1}{h}}\right].$$

Therefore we can easily find

$$\frac{\partial u}{\partial z}\bigg|_{z=0} = \frac{3q}{h^2\left(1 + 3\frac{\delta_1}{h}\right)},$$

16

and

$$\int_0^h u^2 \, dz = \frac{9}{4} \frac{q^2}{h^6 \left(1 + 3\frac{\delta_1}{h}\right)^2} \int_0^h \left(z(2h - z) + 2\delta h\right)^2 \, dz,$$

$$= \frac{9}{4} \frac{q^2}{h^6 \left(1 + 3\frac{\delta_1}{h}\right)^2} \left(\frac{8}{15} h^5 + \frac{8}{3} \delta_1 h^4 + 4\delta_1^2 h^3\right),$$

$$= \frac{6}{5} \frac{q^2}{h \left(1 + 3\frac{\delta_1}{h}\right)^2} \left(1 + \frac{5\delta_1}{h} + \frac{15\delta_1^2}{2h^2}\right),$$

$$= \frac{6}{5} \frac{q^2}{h} \left(\frac{1 + \frac{5\delta_1}{h} + \frac{15\delta_1^2}{2h^2}}{\left(1 + 3\frac{\delta_1}{h}\right)^2}\right).$$

Using these two new facts, 2.3.16 becomes

$$\delta Re \left[\frac{\partial q}{\partial t} + \frac{6}{5} \frac{\partial}{\partial x}\left(\frac{q^2}{h}\left(\frac{1 + \frac{5\delta_1}{h} + \frac{15\delta_1^2}{2h^2}}{\left(1 + 3\frac{\delta_1}{h}\right)^2}\right)\right)\right] = -3\delta h \cot \beta \frac{\partial h}{\partial x} + 3h - \frac{3q}{h^2\left(1 + 3\frac{\delta_1}{h}\right)},$$

$$\implies \frac{\partial q}{\partial t} + \frac{\partial}{\partial x}\left(\frac{6}{5}\frac{q^2}{h}\left(\frac{1 + \frac{5\delta_1}{h} + \frac{15\delta_1^2}{2h^2}}{\left(1 + 3\frac{\delta_1}{h}\right)^2}\right) + \frac{3}{2}\frac{\cot \beta}{Re}h^2\right) = \frac{3h}{\delta Re}\left(1 - \frac{q}{h^3\left(1 + 3\frac{\delta_1}{h}\right)}\right).$$

Thus the Integral Boundary Layer (IBL) equations are

$$\frac{\partial h}{\partial t} + \frac{\partial q}{\partial x} = 0, \tag{2.3.17}$$

$$\frac{\partial q}{\partial t} + \frac{\partial}{\partial x}\left(\frac{6}{5}\frac{q^2}{h}\left(\frac{1 + \frac{5\delta_1}{h} + \frac{15\delta_1^2}{2h^2}}{\left(1 + 3\frac{\delta_1}{h}\right)^2}\right) + \frac{3}{2}\frac{\cot \beta}{Re}h^2\right) = \frac{3h}{\delta Re}\left(1 - \frac{q}{h^3\left(1 + 3\frac{\delta_1}{h}\right)}\right). \tag{2.3.18}$$

Note that these equations have all of the boundary conditions incorporated and there is no more z-dependence. We can understand the flow in terms of just two variables, the height $h(x, t)$ and the flow rate $q(x, t)$. This simplification will also make numerical simulation much simpler since we do not have to include complex boundary conditions in our code. All we will have to do is fix the flow parameters, add initial conditions, and see how h and q evolve in time.

Chapter 3

Linear Stability Analysis

3.1 Linearization

In this section, we want to predict when the flow becomes unstable. That is, if we perturb uniform flow, does the perturbation grow or decay with time. First we need to actually find the steady-state flow, denoted by h_s and q_s. We set $\frac{\partial}{\partial t} = \frac{\partial}{\partial x} = 0$ and notice equation 2.3.18 becomes

$$0 = 1 - \frac{q_s}{h_s^3 \left(1 + 3\frac{\delta_1}{h_s}\right)},$$

$$\implies q_s = h_s^3 \left(1 + 3\frac{\delta_1}{h_s}\right).$$

So if $h_s = 1$ then $q_s = 1 + 3\delta_1$. We will now perturb the steady-state flow as follows

$$h = 1 + \tilde{h},$$
$$q = 1 + 3\delta_1 + \tilde{q}, \tag{3.1.1}$$

where $\tilde{h} \ll 1$ and $\tilde{q} \ll 1$.

Now we will substitute the steady-state and perturbations 3.1.1 into the IBL model 2.3.18 piece by piece. From the left side of 2.3.18 we see

$$\frac{q^2}{h} \left(\frac{1 + \frac{5\delta_1}{h} + \frac{15\delta_1^2}{2h^2}}{\left(1 + 3\frac{\delta_1}{h}\right)^2} \right) \longrightarrow \frac{(1 + 3\delta_1 + \tilde{q})^2}{1 + \tilde{h}} \left(\frac{1 + \frac{5\delta_1}{1+\tilde{h}} + \frac{15\delta_1^2}{2(1+\tilde{h})^2}}{(1 + 3\frac{\delta_1}{1+\tilde{h}})^2} \right). \tag{3.1.2}$$

We take the Taylor expansion of each piece and only retain terms that have perturbations of order one. So we have

$$\frac{1 + \frac{5\delta_1}{1+\tilde{h}} + \frac{15\delta_1^2}{2(1+\tilde{h})^2}}{(1+\tilde{h})(1+3\frac{\delta_1}{1+\tilde{h}})^2} \approx \frac{15\delta_1^2 + 10\delta_1 + 2}{2(1+3\delta_1)^2} - \frac{45\delta_1^3 + 45\delta_1^2 + 14\delta_1 + 2}{2(1+3\delta_1)^3}\tilde{h},$$

and

$$(1 + 3\delta_1 + \tilde{q})^2 \approx \left[(1+3\delta_1)^2 + 2(1+3\delta_1)\tilde{q}\right].$$

Therefore 3.1.2 becomes

$$\frac{15\delta_1^2 + 10\delta_1 + 2}{2} - \frac{45\delta_1^3 + 45\delta_1^2 + 14\delta_1 + 2}{2(1+3\delta_1)}\tilde{h} + \frac{15\delta_1^2 + 10\delta_1 + 2}{1+3\delta_1}\tilde{q}. \qquad (3.1.3)$$

Let

$$\lambda = \frac{15\delta_1^2 + 10\delta_1 + 2}{1+3\delta_1},$$

then we can simplify 3.1.3 as follows

$$\frac{15\delta_1^2 + 10\delta_1 + 2}{2} - \frac{30\delta_1^2 + 20\delta_1 + 4}{2(1+3\delta_1)}\tilde{h} - \frac{45\delta_1^3 + 15\delta_1^2 - 6\delta_1 - 2}{2(1+3\delta_1)}\tilde{h} + \lambda\tilde{q},$$

$$= \frac{15\delta_1^2 + 10\delta_1 + 2}{2} - \lambda\tilde{h} - \frac{15\delta_1^2 - 2}{2}\tilde{h} + \lambda\tilde{q},$$

$$= \frac{15\delta_1^2 + 10\delta_1 + 2}{2} + \lambda\tilde{q} - \left[1 - \lambda - \frac{15}{2}\delta_1^2\right]\tilde{h}. \qquad (3.1.4)$$

Next we look at a different piece of the second IBL equation 2.3.18 and use the same procedure

$$\frac{q}{h^3\left(1+3\frac{\delta_1}{h}\right)} \longrightarrow \frac{1 + 3\delta_1 + \tilde{q}}{(1+\tilde{h})^3\left(1+3\frac{\delta_1}{1+\tilde{h}}\right)},$$

$$\approx (1 + 3\delta_1 + \tilde{q})(1 - 3\tilde{h})\frac{1}{1+3\delta_1}\left(1 + \frac{3\delta_1}{(1+3\delta_1)}\tilde{h}\right),$$

$$\approx \left(1 + \frac{\tilde{q}}{1+3\delta_1}\right)(1 - 3\tilde{h} + \frac{3\delta_1}{(1+3\delta_1)}\tilde{h}),$$

$$= \left(1 + \frac{\tilde{q}}{1+3\delta_1}\right)\left(1 - 3\frac{1+2\delta_1}{1+3\delta_1}\tilde{h}\right),$$

$$= 1 + \frac{\tilde{q}}{1+3\delta_1} - 3\frac{1+2\delta_1}{1+3\delta_1}\tilde{h}.$$

19

So the RHS of the 2.3.18 equation becomes

$$\frac{3(1+\tilde{h})}{\delta Re}\left(1 - 1 - \frac{\tilde{q}}{1+3\delta_1} + 3\frac{1+2\delta_1}{1+3\delta_1}\tilde{h}\right),$$

$$\approx \frac{3}{\delta Re(1+3\delta_1)}\left(3(1+2\delta_1)\tilde{h} - \tilde{q}\right). \tag{3.1.5}$$

It is easy to see that only the perturbations remain, when we plug 3.1.1 into 2.3.17. Using 3.1.4 and 3.1.5, the linearized IBL equations are given by

$$\frac{\partial \tilde{h}}{\partial t} + \frac{\partial \tilde{q}}{\partial x} = 0, \tag{3.1.6}$$

$$\frac{\partial \tilde{q}}{\partial t} + \frac{6}{5}\lambda\frac{\partial \tilde{q}}{\partial x} + \frac{6}{5}\left[1 - \lambda - \frac{15}{2}\delta_1^2\right]\frac{\partial \tilde{h}}{\partial x} + \frac{3\cot\beta}{Re}\frac{\partial \tilde{h}}{\partial x}$$

$$= \frac{3}{\delta Re(1+3\delta_1)}\left(3(1+2\delta_1)\tilde{h} - \tilde{q}\right). \tag{3.1.7}$$

3.2 Wave Propagation

Next we set the perturbations to

$$\tilde{h} = h_0 e^{\gamma t} e^{ikx} \quad \text{and} \quad \tilde{q} = q_0 e^{\gamma t} e^{ikx}, \tag{3.2.1}$$

which describe wave solutions. Here $\gamma = \gamma_R + i\gamma_I$ is a complex-valued parameter where γ_R is the growth rate. We know that $\gamma_R > 0 \implies$ a disturbance will grow in time, $\gamma_R < 0 \implies$ a disturbance will decay in time, and $\gamma_R = 0 \implies$ neutral stability. We substitute these wave solutions into the first IBL equation 2.3.17 which results in

$$h_0\gamma e^{\gamma t}e^{ikx} + q_0 e^{\gamma t}ike^{ikx} = 0,$$

$$\implies h_0 = -\frac{ik}{\gamma}q_0. \tag{3.2.2}$$

Now we substitute the wave solutions 3.2.1 into the second IBL equation 2.3.18 and divide out the exponentials to get

$$(\gamma q_0) + \frac{6}{5}\lambda(ikq_0) + \frac{6}{5}\left[1 - \lambda - \frac{15}{2}\delta_1^2\right](ikh_0) + \frac{3\cot\beta}{Re}(ikh_0)$$

$$= \frac{3}{\delta Re(1+3\delta_1)}\left(3(1+2\delta_1)h_0 - q_0\right).$$

Next we substitute 3.2.2 in and factor out q_0 to get

$$\left[\gamma + \frac{6}{5}\lambda ik + \frac{6}{5}\left[1 - \lambda - \frac{15}{2}\delta_1^2\right]\frac{k^2}{\gamma} + \frac{3\cot\beta}{Re}\frac{k^2}{\gamma}\right.$$
$$\left. + \frac{3}{\delta Re(1 + 3\delta_1)}\left(3(1 + 2\delta_1)\frac{ik}{\gamma} + 1\right)\right]q_0 = 0. \tag{3.2.3}$$

For a non-trivial solution with $q_0 \neq 0$, we must have the expression inside the brackets equal to 0. To find the onset of the instability we set

$$\gamma = \gamma_R + i\gamma_I = 0 - ick. \tag{3.2.4}$$

Here c is the phase speed which we can see from the following relation:

$$e^{\gamma t}e^{ikx} = e^{\gamma_R t}e^{ikx}e^{i\gamma_I t} = e^{\gamma_R t}e^{i(kx + \gamma_I t)}.$$

Clearly $e^{\gamma_R t}$ describes exponential growth and decay while $e^{i(kx + \gamma_I t)}$ is a travelling wave. Compare this equation for a travelling wave to the more conventional form $e^{i(kx - \omega t)}$, so $\gamma_I = -\omega = -ck$. Using 3.2.4 on the bracketed part of 3.2.3, we need

$$ik\left[-c + \frac{6}{5}\lambda + \frac{6}{5}\left[1 - \lambda - \frac{15}{2}\delta_1^2\right]\frac{1}{c} + \frac{3\cot\beta}{Re}\frac{1}{c}\right]$$
$$+ \frac{3\cot\beta}{\delta Re}\left[1 - \frac{3(1 + 2\delta_1)}{c}\right] = 0.$$

Note that the first term is the imaginary part and the second term is the real part. Setting the real part to zero yields

$$c = 3(1 + 2\delta_1),$$

and plugging this into the imaginary part and setting it to zero results in

$$0 = -3(1 + 2\delta_1) + \frac{6}{5}\lambda + \frac{2}{5(1 + 2\delta_1)}\left[1 - \lambda - \frac{15}{2}\delta_1^2\right] + \frac{\cot\beta}{Re(1 + 2\delta_1)},$$
$$\implies 0 = -3(1 + 2\delta_1)^2 + \frac{6}{5}(1 + 2\delta_1)\lambda + \frac{1}{5}[2 - 2\lambda - 15\delta_1^2] + \frac{\cot\beta}{Re},$$
$$\implies 0 = -(1 + \delta_1)(1 + 3\delta_1) + \frac{\cot\beta}{Re}.$$

Therefore we have

$$Re = Re_{crit} = \frac{\cot \beta}{(1 + \delta_1)(1 + 3\delta_1)}. \tag{3.2.5}$$

This describes the tipping point when the perturbations begin to grow instead of decay. We call this the critical Reynolds number and denote it by Re_{crit}. We now have a way to predict when the flow becomes unstable as a function of the slip-length δ_1. It is also clear from this expression that a porous boundary destabilizes the flow since any positive value of δ_1 will decrease Re_{crit} when compared to the non-porous case. It is worth comparing our prediction to the existing literature.

If we were to set $\delta_1 = 0$, or equivalently, to perform all of the above analysis with the no-slip condition $u = 0$ at $z = 0$, we would arrive at the simple expression $Re_{crit} = \cot \beta$. But the no-slip case has been studied extensively over the years using more sophisticated techniques as in [1], [2], and [3]. These all show the well-known theoretical result $Re_{crit} = \frac{5}{6} \cot \beta$ which has also been verified by experiment [4]. This indicates that our result in 3.2.5 is already an overestimate. We are missing the fraction $\frac{5}{6}$. But more recent work in [15], [16], and [17] has produced an entirely different expression. It is given by

$$Re_{crit} = \frac{5}{6} \cot \beta \left[\frac{1 + 3\delta_1}{1 + 6\delta_1 + \frac{25}{2}\delta_1^2} \right]. \tag{3.2.6}$$

In [15] the authors use a much more sophisticated second-order weighted-residual model to derive this expression. This weighted-residual method, originally from [5] & [6] has led to many advancements in the study of flow down an incline. We anticipate that 3.2.6 is more accurate. It also includes the fraction $\frac{5}{6}$ missing from 3.2.5. While the model in [15] does have these notable strengths, it also has notable downsides. It is more complicated to derive and simulate and does not have the exact solution step that we will see in our model.

Chapter 4

Numerical Method

4.1 Overview

We want to solve the first-order IBL equations

$$\frac{\partial h}{\partial t} + \frac{\partial q}{\partial x} = 0, \tag{4.1.1}$$

$$\frac{\partial q}{\partial t} + \frac{\partial}{\partial x}\left(\frac{6}{5}\frac{q^2}{h}\left(\frac{1 + \frac{5\delta_1}{h} + \frac{15\delta_1^2}{2h^2}}{\left(1 + 3\frac{\delta_1}{h}\right)^2}\right) + \frac{3}{2}\frac{\cot\beta}{Re}h^2\right) = \frac{3h}{\delta Re}\left(1 - \frac{q}{h^3\left(1 + 3\frac{\delta_1}{h}\right)}\right).$$

Note that the flow is completely characterized by the dimensionless parameters: δ, δ_1, $\cot\beta$, and Re.

We establish a computational domain $0 \le x \le L$ and apply periodic boundary conditions (BC), $h(x = 0, t) = h(x = L, t)$ and $q(x = 0, t) = q(x = L, t)$. We use initial conditions (IC) of a perturbed steady-state solution given by

$$h(x, t = 0) = 1 + \varepsilon\sin\left(\frac{2\pi x}{L}\right),$$

$$q(x, t = 0) = 1 + 3\delta_1 + \varepsilon\sin\left(\frac{2\pi x}{L}\right). \tag{4.1.2}$$

It can be shown that perturbations with infinite wavelength are the most unstable [17]. So in this case we choose a perturbation with longest possible wavelength, that of the

computational domain.

In order to solve the IBL equations 4.1.1 above, we use a fractional-step method. The first step is to solve the hyperbolic system given by

$$\frac{\partial h}{\partial t} + \frac{\partial q}{\partial x} = 0,$$

$$\frac{\partial q}{\partial t} + \frac{\partial}{\partial x}\left(\frac{6}{5}\frac{q^2}{h}\left(\frac{1 + \frac{5\delta_1}{h} + \frac{15\delta_1^2}{2h^2}}{\left(1 + 3\frac{\delta_1}{h}\right)^2}\right) + \frac{3}{2}\frac{\cot\beta}{Re}h^2\right) = 0, \tag{4.1.3}$$

using 4.1.2 as the initial condition. Note that in 4.1.3 we set the source term on the RHS to 0. This will be solved over a time step Δt. Then the output for the first step will be used as an initial condition for the second step.

In the second step we now deal with the source term and solve

$$\frac{\partial q}{\partial t} = \frac{3h}{\delta Re}\left(1 - \frac{q}{h^3\left(1 + 3\frac{\delta_1}{h}\right)}\right). \tag{4.1.4}$$

Note that in this step h remains constant since the RHS of the first IBL equation is 0, so it has no source.

4.2   Step 1

Equations 4.1.3 are a non-linear system of hyperbolic conservation laws. We express them in vector form as

$$\frac{\partial \vec{u}}{\partial t} + \frac{\partial \vec{F}}{\partial x} = 0, \tag{4.2.1}$$

where

$$\vec{u} = \begin{bmatrix} h \\ q \end{bmatrix} \qquad \text{and} \qquad \vec{F} = \begin{bmatrix} q \\ \frac{6}{5}\frac{q^2}{h}\left(\frac{1 + \frac{5\delta_1}{h} + \frac{15\delta_1^2}{2h^2}}{\left(1 + 3\frac{\delta_1}{h}\right)^2}\right) + \frac{3}{2}\frac{\cot\beta}{Re}h^2 \end{bmatrix}. \tag{4.2.2}$$

24

We will solve this using the MacCormack method [20]. It is a second-order finite difference predictor-corrector algorithm given by

$$\vec{u}_j^* = \vec{u}_j^n - \frac{\Delta t}{\Delta x} \left[\vec{F}\left(\vec{u}_{j+1}^n\right) - \vec{F}\left(\vec{u}_j^n\right) \right], \tag{4.2.3}$$

$$\vec{u}_j^{n+1} = \frac{1}{2}\left(\vec{u}_j^n + \vec{u}_j^*\right) - \frac{\Delta t}{2\Delta x}\left[\vec{F}\left(\vec{u}_j^*\right) - \vec{F}\left(\vec{u}_{j-1}^*\right)\right]. \tag{4.2.4}$$

Here Δx is the uniform grid spacing, Δt is the time step, and $\vec{u}_j^n = \vec{u}(x_j, t_n)$. A proper stability analysis would be exceedingly complicated due to the highly non-linear nature of the IBL equations. To compensate we use a very small time step to guarantee numerical stability. We choose computational parameters $\Delta x = 0.01$ and $\Delta t = 0.00005$ throughout our simulations.

4.3 Step 2

The second step is a linear separable ODE which we can solve exactly. We use $q = q_0$ as an initial condition and have $h = h_0$ since it is constant in this step. We have

$$\frac{dq}{dt} = \frac{3h}{\delta Re}\left(1 - \frac{q}{h^3\left(1 + 3\frac{\delta_1}{h}\right)}\right), \tag{4.3.1}$$

$$\implies \frac{dq}{\left(1 - \frac{q}{h^3\left(1+3\frac{\delta_1}{h}\right)}\right)} = \frac{3h}{\delta Re}dt, \tag{4.3.2}$$

$$\implies -h^3\left(1 + 3\frac{\delta_1}{h}\right)\log\left[1 - \frac{q}{h^3\left(1+3\frac{\delta_1}{h}\right)}\right] = \frac{3ht}{\delta Re} + c, \tag{4.3.3}$$

$$\implies 1 - \frac{q}{h^3\left(1+3\frac{\delta_1}{h}\right)} = Ke^{-\Gamma}, \tag{4.3.4}$$

$$\implies q = h^3\left(1 + 3\frac{\delta_1}{h}\right)\left[1 - Ke^{-\Gamma}\right], \tag{4.3.5}$$

where $\Gamma = \frac{3t}{\delta Reh^2\left(1+3\frac{\delta_1}{h}\right)}$. Now we use the initial condition $q = q_0$ at $t = 0$ to get

$$q_0 = h_0^3\left(1 + 3\frac{\delta_1}{h_0}\right)\left[1 - K\right], \tag{4.3.6}$$

$$\implies K = 1 - \frac{q_0}{h_0^3\left(1 + \frac{\delta_1}{h_0}\right)}. \tag{4.3.7}$$

So our solution to the ODE is

$$q = h_0^3 \left(1 + \frac{\delta_1}{h_0} \right) - \left[h_0^3 \left(1 + \frac{\delta_1}{h_0} \right) - q_0 \right] e^{-\Gamma}. \qquad (4.3.8)$$

The fact that we can solve the second step exactly is a beautiful aspect of these particular IBL equations. If we chose a different complication besides a porous boundary or used a second-order model as in [15], we would have to solve this step numerically.

Chapter 5

Results and Discussion

With our numerical scheme established, we are ready to investigate what this flow looks like and what happens after it becomes unstable. Unless stated otherwise, we use $\cot \beta = 1$ in our simulations which is a 45-degree angle.

Consider an example with the other flow parameters $\delta = 0.1$, $\epsilon = 0.1$, $L = 2$, and $\delta_1 = 0$. Note that this is the case with an impermeable boundary. Our model predicts a critical Reynolds number of $Re_{crit} = 1$. We choose one case with $Re = 0.5$ and another with $Re = 1.0$. The former should be stable and we anticipate that it will decay back to steady state, while the latter should be unstable. We run the simulation for 15 units of time which can be seen in Figure 5.1.

The stable scenario behaves exactly as expect and decays back to steady state. For the unstable case we see three distinct spikes and if we were to continue the simulation they would stay in this fixed position travelling down the incline. The spikes with height greater than 3 are certainly unphysical since we started with a perturbation of just 0.1 and the fluid height was essentially 1 everywhere. But it is important to remember that this is a first-order model which eliminated one of our terms that makes up viscosity. If we had the full influence of velocity, it would make the height of the spikes shorter, wider, and closer to reality.

In Figure 5.2 we can see how the spikes form with the introduction of a porous bottom. We see many small peaks develop which come together to form four larger peaks of equal height. Note that there are four spikes after 15 units of time, while in the last example there were only three. We can attribute this to the destabilizing effect of a porous bottom
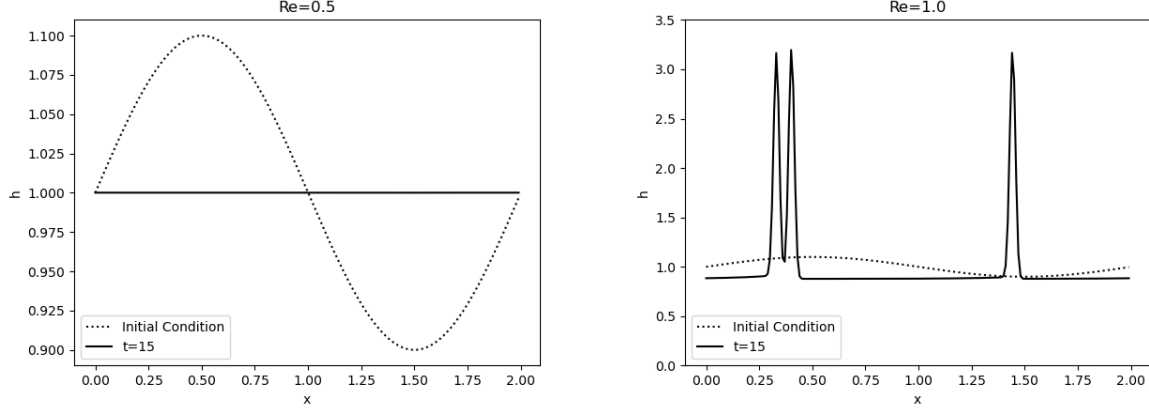
Figure 5.1: Simulations with $\delta = 0.1$, $\epsilon = 0.1$, $L = 2$, and $\delta_1 = 0$

which we concluded in our linear stability analysis. Again the height is unphysical but we are neglecting viscosity. It is also important to point out that our numerical method conserves volume. If we integrated across the fluid layer at each time step, we would realize that there is always the same amount of fluid. The mass that contributes to the peaks clearly comes from the flat part of the flow.

Another interesting aspect of this system is how the Reynolds number affects the destabilized flow. We can actually control the number of spikes we get in the end by increasing or decreasing Re. Using the same flow parameters as above, we can determine numerically that the critical Reynolds number is in the range $(0.74, 0.75)$. Choosing 0.75 produces only one spike, but we can add spikes by increasing this value as seen in Figure 5.3. In general, a higher Reynolds number results in a fluid that is more likely to be turbulent and further from stable, laminar flow. Our observation of more spikes for a larger Reynolds agrees with this idea.

We are now ready to see how our theoretical predictions compare to our numerical results. We are mainly interested in the influence of porosity and how varying δ_1 affects Re_{crit}. But before we can vary δ_1, we must fix our other parameters. In Table 5.1 we test several combinations of parameter values.
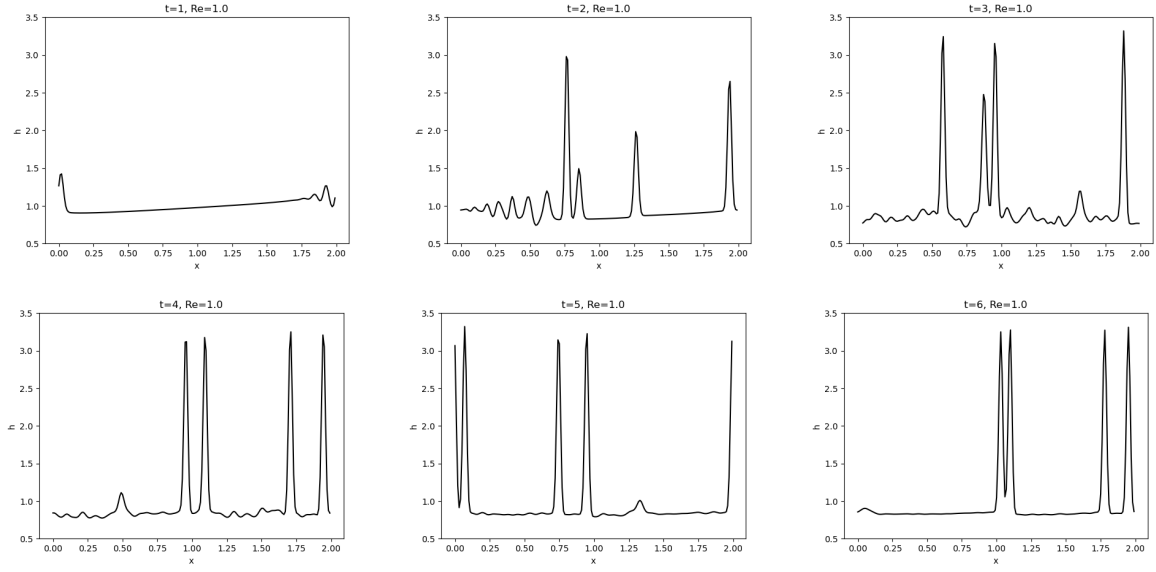
Figure 5.2: Simulations with $\delta = 0.1$, $\epsilon = 0.1$, $L = 2$, and $\delta_1 = 0.1$

δ	ϵ	L	Re$_{crit}$	δ	ϵ	L	Re$_{crit}$
0.1	0.1	2	(0.89, 0.90)	0.05	0.1	2	(0.87, 0.88)
		4	(0.88, 0.89)			4	(0.86, 0.87)
		6	(0.88, 0.89)			6	(0.85, 0.86)
		8	(0.87, 0.88)			8	(0.84, 0.84)
	0.05	2	(0.93, 0.94)		0.05	2	(0.92, 0.93)
		4	(0.93, 0.94)			4	(0.91, 0.92)
		6	(0.92, 0.93)			6	(0.91, 0.92)
		8	(0.91, 0.92)			8	(0.90, 0.91)
	0.025	2	(0.96, 0.97)		0.025	2	(0.96. 0.97)
		4	(0.96, 0.97)			4	(0.95, 0.96)
		6	(0.96, 0.97)			6	(0.95. 0.96)
		8	(0.95, 0.96)			8	(0.94, 0.95)

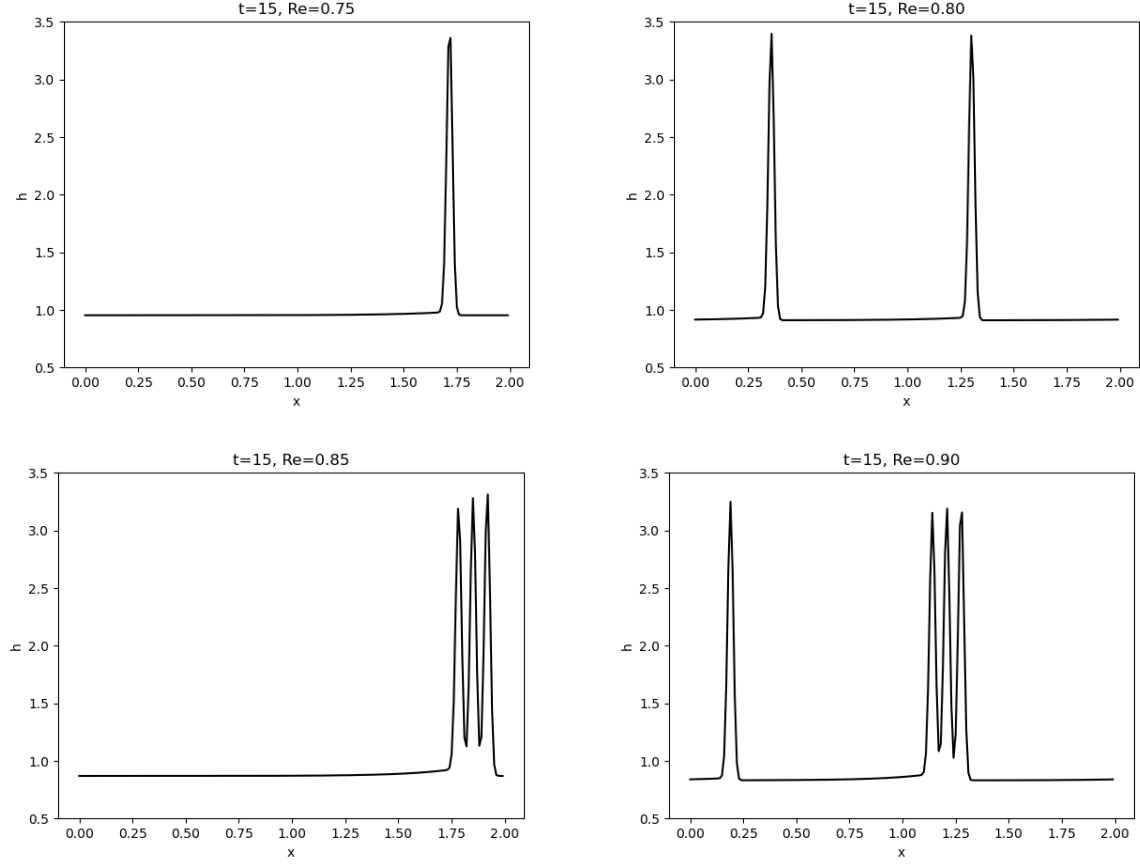Table 5.1: Influence of δ, ϵ, and L on Re_{crit}

29

Figure 5.3: Simulations with $\delta = 0.1$, $\epsilon = 0.1$, $L = 2$, and $\delta_1 = 0.1$

We notice increasing the length has barely any effect on the critical Reynolds number. Also, as we extend the domain we get less numerical stability and we are forced to change either the time step or the spatial domain to accommodate. We want to avoid doing this as it makes the simulation more expensive and there seems to be no advantage. We also notice that $\delta = 0.1$ results in smaller changes to Re_{crit} as we vary ϵ. Although any value for ϵ seems reasonable, in theory we want our perturbation to be infinitesimal. So choosing $\epsilon = 0.1$ may be slightly large, while taking $\epsilon = 0.025$ takes far longer for the flow to become unstable. For our study of porosity we fix the parameters $\delta = 0.1$, $\epsilon = 0.05$, and $L = 2$.

The results of our numerical experiments are displayed in Figure 5.4. But it is important to remember that we are not testing our predictions with the full dynamics of the Navier-

Stokes equations. Instead we are simulating the first-order IBL equations 4.1.1 and plotting the predictions from linear theory 3.2.5.
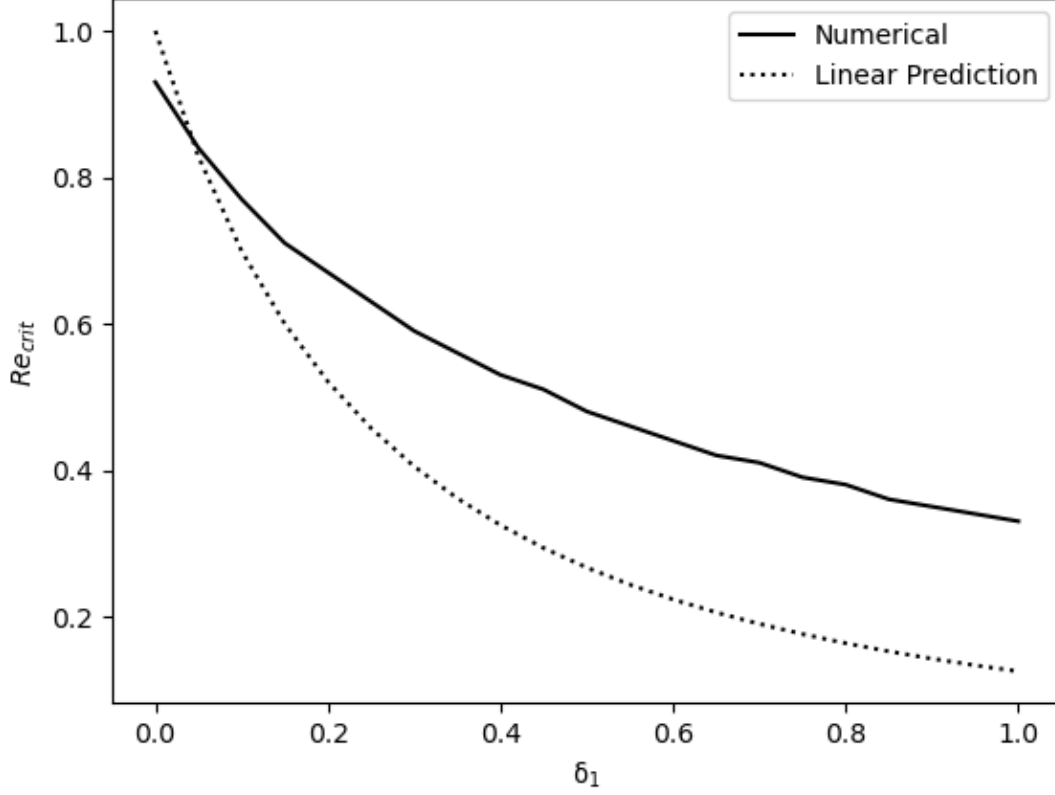

Figure 5.4: Re_{crit} as a function of δ_1 from first-order model

Immediately we notice that our theoretical predictions offer a decent estimate for stability, but overall under-predict the critical Reynolds number. It appears to be best for small slip-length $\delta < 0.1$. The linear prediction seems to decays too quickly and has too steep of a slope. It is also worth comparing our first-order model and linearization to a completely different model.
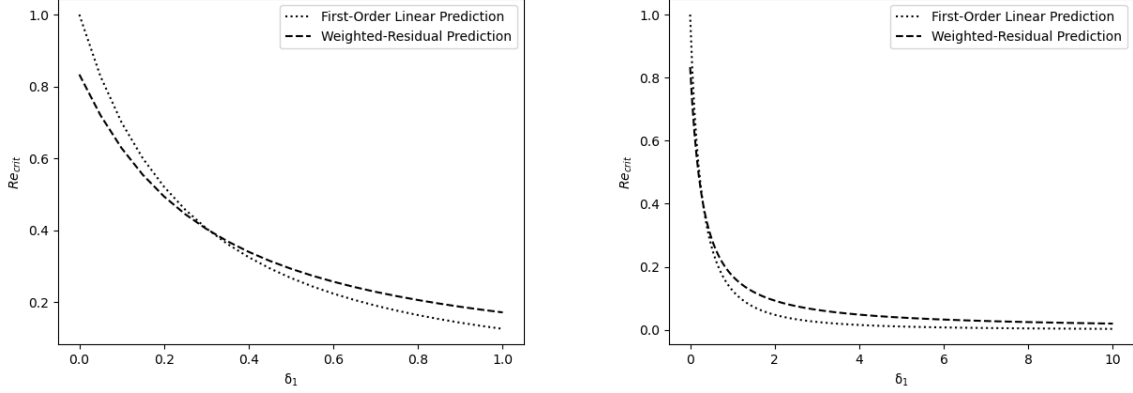
Figure 5.5: First-order IBL model and Weighted-Residual Model

We see that the agreement between these two models is very good for $\delta_1 < 1$. The largest difference is at $\delta_1 = 0$ where the first-order model predicts 1 since the expression does not include the fraction $\frac{5}{6}$. Now the slip-length is not restricted to small values and is only bound by the size of the domain. We can see some larger scale behaviour in the plot on the right. Both models have an asymptote at 0, but the first-model decays too quickly and differs the most at about $\delta_1 = 2$. So for very large values of δ_1 both models will predict almost the same value.

Chapter 6

Conclusion

In this work we studied 2D gravity-driven flow down a porous incline. This is one of many variations of a classic problem in fluid dynamics. To better understand the problem, we have developed the first-order Integrated Boundary Layer model. This is a relatively simple model with only two governing equations. We were then able to linearize the equations and predict the destabilizing critical Reynolds number as a function of slip-length and angle of inclination. We simulated the IBL equations numerically with small perturbations and observe low Reynolds number flow to quickly return to steady-state. For high Reynolds number flow we see the perturbation produce many small waves which gather together into many large spikes that become a permanent feature of the flow.

Overall there is good agreement between our predictions and our numerical results. However, this problem has been studied in depth by others and there exist better models. One example is given by a weighted-residual model. This is much more mathematically complex, which makes it harder to derive and more expensive to simulate. Although it is known to give better agreement between stability predictions and numerical results, the added complexity and necessary computational power may not be worth it. Depending on the physical system, relevant flow parameters, and necessary accuracy, the IBL equations could be a valuable tool in modelling this kind of flow.

References

[1] Benjamin, T. (1957). Wave formation in laminar flow down an inclined plane. Journal of Fluid Mechanics, 2(6), 554-573.

[2] Yih, C.-S. (1963). Stability of liquid flow down an inclined plane. Physics of Fluids, 6, 321.

[3] Benney, D.J. (1966). Long Waves on Liquid Films. Journal of Mathematics and Physics, 45, 150-155.

[4] Liu, J., Paul, J., & Gollub, J. (1993). Measurements of the primary instabilities of film flows. Journal of Fluid Mechanics, 250, 69-101.

[5] Ruyer-Quil, C. & Manneville, P. (2000). Improved modelling of flows down inclined planes. European Physical Journal B, 15, 357.

[6] Ruyer-Quil C. & Manneville, P. (2002). Further accuracy and convergence results on the modelling of flows down inclined planes by weighted-residual approximations. Physics of Fluids, 14, 170.

[7] Beavers, G.S. & Joseph, D.D. (1967). Boundary conditions at a naturally permeable wall. Journal of Fluid Mechanics, 30, 197.

[8] Shkadov, V.Y. (1967). Wave conditions in flow of thin layer of a viscous liquid under the action of gravity. Izv. Akad. Nauk SSSR, Mekh. Zhidk. Gaza 1, 43.

[9] Pascal, J.P., D'Alessio, S.J.D., & Zafar, S.R. (2019). The instability of liquid films with temperature-dependent properties flowing down a heated incline. AIMS Mathematics, 4(6): 1700-1720.

[10] Ruyer-Quil, C., Scheid,B., Kalliadasis, S., Velarde, M.G., & Zeytounian, R.Kh. (2005). Thermocapillary long waves in a liquid film flow. Part 1. Low-dimensional formulation. Journal of Fluid Mechanics, 538, 199.

[11] Scheid, B., Ruyer-Quil, C., Kalliadasis, S., Velarde, M.G., & Zeytounian, R.Kh. (2005). Thermocapillary long waves in a liquid film flow. Part 2. Linear stability and nonlinear waves. Journal of Fluid Mechanics, 538, 223.

[12] D'Alessio, S.J.D., Pascal, J.P., Jasmine, H.A., & Ogden, K.A. (2010). Film flow over heated wavy inclined surfaces. Journal of Fluid Mechanics, 665, 418.

[13] D'Alessio, S.J.D., Seth, C., & Pascal, J.P. (2014). The effects of variable fluid properties on thin film stability. Physics of Fluids, 26, 122105.

[14] D'Alessio, S.J.D., Pascal, J.P., Ellaban, E., & Ruyer-Quil, C. (2020). Marangoni instabilities associated with heated surfactant-laden falling films. Journal of Fluid Mechanics, 887, 10.

[15] Ogden, K., D'Alessio, S.J.D., & Pascal, J.P. (2011). Gravity-driven flow over heated, porous, wavy surfaces. Physics of Fluids. 23.

[16] Pascal, J.P. & D'Alessio, S.J.D. (2010). Instability in gravity-driven flow over uneven permeable surfaces. International Journal of Multiphase Flow. 36, 449-459.

[17] Pascal, J.P. (1999). Linear stability of fluid flow down a porous inclined plane. Journal of Physics D, 32, 417.

[18] Kundu, P., Cohen, I., & Dowling D. (2016). Fluid Mechanics. Academic Press.

[19] D'Alessio, S.J.D. (2018). Flow past a slippery cylinder: part 1—circular cylinder. Acta Mechanica, 229, 3375-3392.

[20] LeVeque, R.J. & Yee, H.C. (1990). A study of numerical methods for hyperbolic conservation laws with stiff source terms. Journal of Computational Physics, 86, 187.